Investigating the loading behaviour of intact and meniscectomy knee joints and the impact on surgical decisions

M. S. Yeoman[1]
1. Continuum Blue Limited, One Caspian Point, Caspian Way, CF10 4DQ, United Kingdom

Introduction

The meniscus is a crescent-shaped fibrocartilaginous structure that lies between the cartilage of the femur and tibia of the knee joint. Two menisci are present in each knee joint, one medial and one lateral, together they cushion and stabilize the knee (see Figure 2). A meniscectomy is the surgical removal of all, or a part of a torn or damaged meniscus. Tears in the menisci are common in knee joint injuries and depending on the location and severity of the tear, orthopaedic surgeons who perform meniscectomies will make surgical decisions based on the age, health and activity level of the patient, as well as the meniscus's ability to heal.

Peripheral (outer rim) tears are highly vascularized and thus have the potential to heal. However, inner rim tears which lack a good blood supply do not tend to heal. The type of inner tear, or damage, often determines whether a tear can be repaired. Longitudinal tears and radial tears are often repairable, depending on their location, while oblique (or flap) and horizontal tears are generally not repairable. In these cases, if the torn pieces of meniscus are causing inflammation and pain, a partial meniscectomy (section of meniscus is excised) may be done. In this case, the surgeon has to decide how much of the meniscus to remove.

In this work an intact (natural, no-defect) knee model was developed from patient specific MRI data, and two partial meniscectomy virtual surgeries of different resection lengths, namely, 30mm and 35mm, based on a typical defect were performed. Numerical modelling of the intact and the two partial meniscectomy models were performed, and used to assess the knee mechanics and loading with variation in defect position and meniscectomy outcome. The results of the partial meniscectomy models where then compared to the intact case, which was used as a reference to evaluate if reducing the resection length of the defect improved knee mechanics and loading toward that of the intact (natural, no-defect) knee reference model.

Additionally, a method of ranking and grading the various virtual surgery options relative to the intact model was implemented, with the aim of helping surgeons to evaluate which surgical procedure is best based on maintaining patient functional mobility.

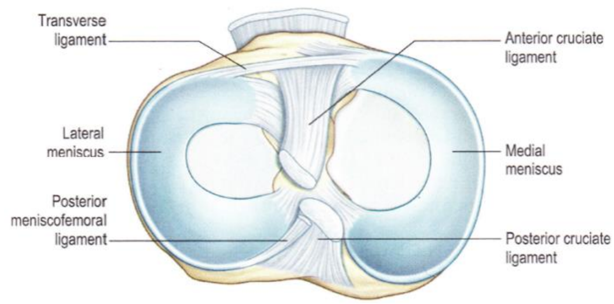

Figure 1: Superior aspect of the medial and lateral menisci in a left knee joint and attachments to tibia from [1]

Patient Specific Data and MRI Segmentation

MRI imaging data was obtained from a 48 year old Caucasian male having a weight of 78kgs, with no previous history of hip, knee or ankle problems. 3D Slicer v4.6 [2-3] software was used to segment the MRI data and obtain the required geometries for the intact knee model, as shown in Figure 2, below.

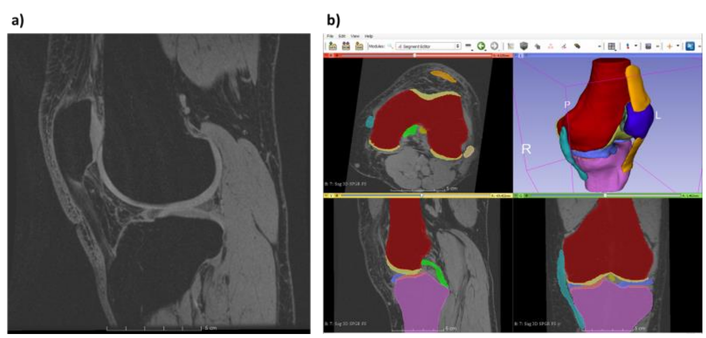

Figure 2: a) MRI image of knee section (sagittal plane) and b) screenshot of 3D Slicer and segmentation of knee region

Model

A literature review of knee kinematics and modelling techniques was preformed [4-17], to assess current methods and techniques utilised in the field. From this review, three models were developed with the appropriate loads, boundary conditions and material relations. The knee domains and features implemented in the model are presented in Figure 3, below.

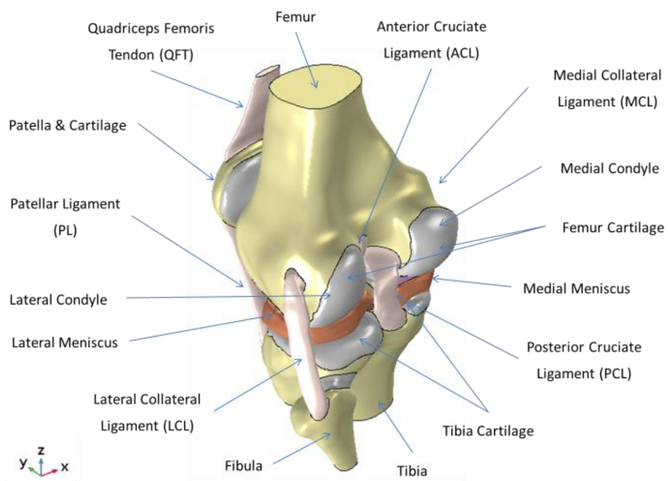

Figure 3: Knee model domains and features developed from segmented MRI data

Defect Size and Location

A defect location was defined on the posterior side of the medial meniscus based on literature. Two virtual partial meniscectomy surgeries where then performed on the intact model, namely a 30mm, and 35mm resection on the posterior side of the medial meniscus. The three models developed included; a) intact (natural, no-defect), b) partial meniscectomy (30mm resection), c) partial meniscectomy (35mm resection). Figure 4 below, displays the difference between these models by presenting the tibia, tibia cartilage (on both medial and lateral sides), the menisci, and the removed defects on the medial meniscus for the two partial meniscectomy models compared to the intact case, from the superior aspect.

Load and boundary conditions

The load and boundary conditions applied to the knee model included two load cases, namely, 1) standing, and 2) walking gait. The standing load case assumes zero rotations or moments being applied to the femur bony components, only an axial load is applied from the inferior surfaces of the tibia and fibula, such that the load is equal to half the axial force of the weight of the patient. The walking gait load case assesses the knee model during a gait cycle (stance and swing).

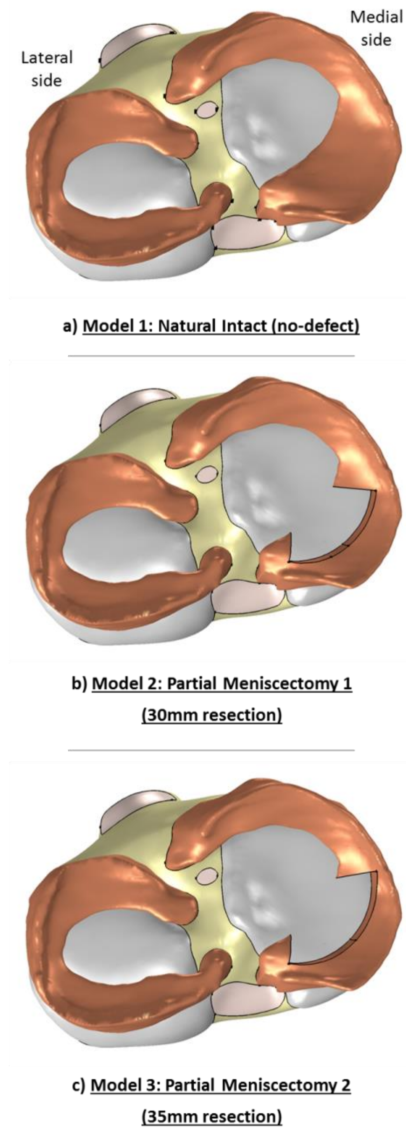

Figure 4: Intact menisci compared to partial meniscectomy models (superior views of menisci, tibia cartilage & tibia)

Rotations, including flexion-extension, internal-external and abduction-adduction were applied to the femur, while the tibia is axially loaded in compression and allowed to freely traverse laterally and in the posterior-anterior direction without rotation. These loads and rotations were implemented in the model similar to the work by Mononen *et al.* (2013)[8]. The applied rotations were based on the mean rotations in the three planes (sagittal, coronal and axial) obtained from the work by Kadaba *et al.* (1990)[16]. The events and phases of a level walking gait cycle[17] and knee motions from Kadaba *et al.* (1990)[16], are presented in Figure 5 below.

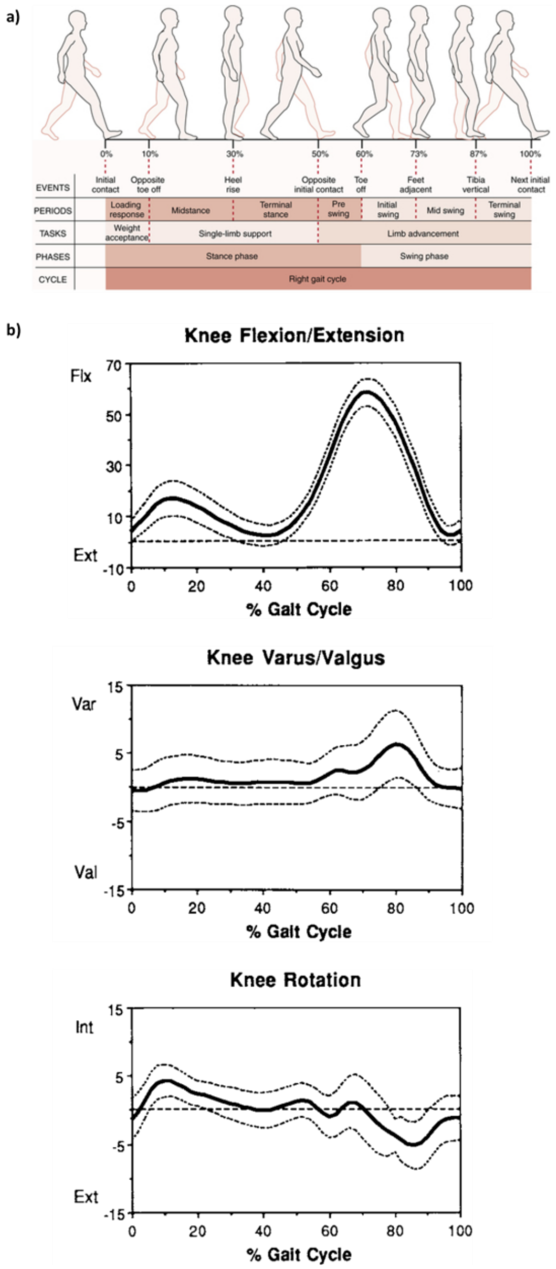

Figure 5: a) Level walking gait cycle events, periods and phases [17], and b) knee motions in the three planes during level walking gait cycle obtained from [16]

In addition to the rotations, distal compressive loads were applied to the model from the tibia and fibula inferior surfaces. These compressive loads are based on the stance phase of the control group data from Sanford *et al.* (2014)[14], which are reported in the reference frame of the segment distal (or tibia) to the knee joint. It was assumed that the stance phase was 61%[14,16] of the gait cycle based on the specific patient gender and the male figures from Kadaba *et al.* (1990)[16]. For the remaining swing phase of the gait cycle the compressive loads were assumed to be constant through the swing cycle. The average weight of the control group was 65.5 kg[14], this was used to normalise the compressive force curves utilised in the model. This compressive force data was adjusted to the weight of specific patient (78kg), from which the MRI dataset was obtained. The stride compressive force curves from Sanford *et al.* (2014)[14] and the normalised gait cycle compressive force curve utilised in the model are presented in Figure 6 below.

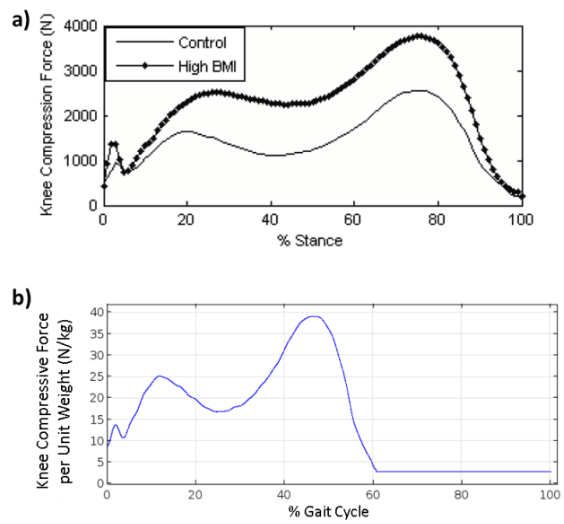

Figure 6: a) Knee compressive loading during stance phase of walking gait cycle from [14], and b) knee compressive load normalised to weight over gait cycle used in model

Contact

Frictionless contact was assumed between all articulating surfaces [6, 8, 12].

Materials Properties

The material models implemented include, hyper-elastic (neo-Hookean), linear orthotropic and isotropic material models. The material models are based on the work by [7, 10-11]. A summary of the material models utilised in the model for each knee component is provided in Table 1 below.

Table 1: Material models utilised in model

Knee bodies	Material Model	Values			
		Density (g/cm^3)	Modulus (MPa)	Poisson's Ratio	Reference
Deformable Bony Components (Femur, Tibia, Fibula & Patella)	Linear elastic (isotropic)	2	15x10^3	0.3	[7]
Articular cartilage	Linear elastic (isotropic)	1	15	0.475	[10]
Menisci♣	Linear elastic (orthotropic)	1.5	E_1: 20 E_2: 120 E_3: 20	ν_{12}: 0.3 ν_{13}: 0.45 ν_{23}: 0.3	[10]
Ligaments♠	Hyper-elastic (neo-Hookean)	1	LCL: 6.06 MCL: 6.43 ACL: 5.83 PCL: 6.06 PL: 5.83 QFT: 5.83	0.45 0.45 0.45 0.45 0.45 0.45	[11]

♣ Direction 1 is radial, 2 is circumferential, and 3 is axial
♠ Refer to Figure 2 for acronyms for specific ligaments

Results

The standing and walking gait cycle load cases were run for the intact and the two partial meniscectomy models. Only the standing load data is presented. Plots of anterior-posterior and lateral-medial displacement magnitudes and principal stresses for the menisci (medial and lateral), and contact pressures and loading patterns for the articulating surfaces were generated and assessed for the various models run. Figure 7 presents the displacement magnitudes between the models on the axial plane (anterior-posterior and lateral-medial displacement) only. From these images, it can be seen that the displacements for the partial meniscectomy models are significantly different from the intact case on both the medial and lateral menisci. However, the conserving 30mm resection model is a closer match to those of the intact case, especially on the medial meniscus, indicating that this should provide a better surgical out-come for the patient.

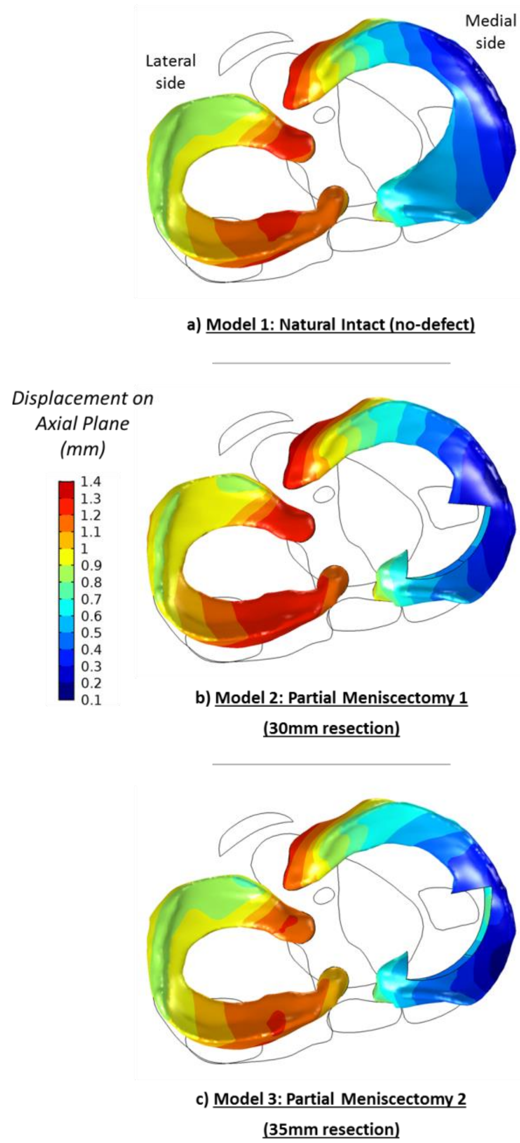

Figure 7: Menisci anterior-posterior and lateral-medial direction displacement magnitudes for standing load case (superior views only)

The contact pressures and loading patterns across the various articulating surfaces are presented in Figure 8. Based on the observed pressure footprint on the lateral side of the knee joint, no significant difference can be seen between the various models. However, a large difference is observed on the medial side of the joint, where again, it can be seen that the contact footprint in the conserving 30mm resection model, is more evenly distributed across the posteromedial side of the medial meniscus, and is again, a closer match to the ideal natural intact case.

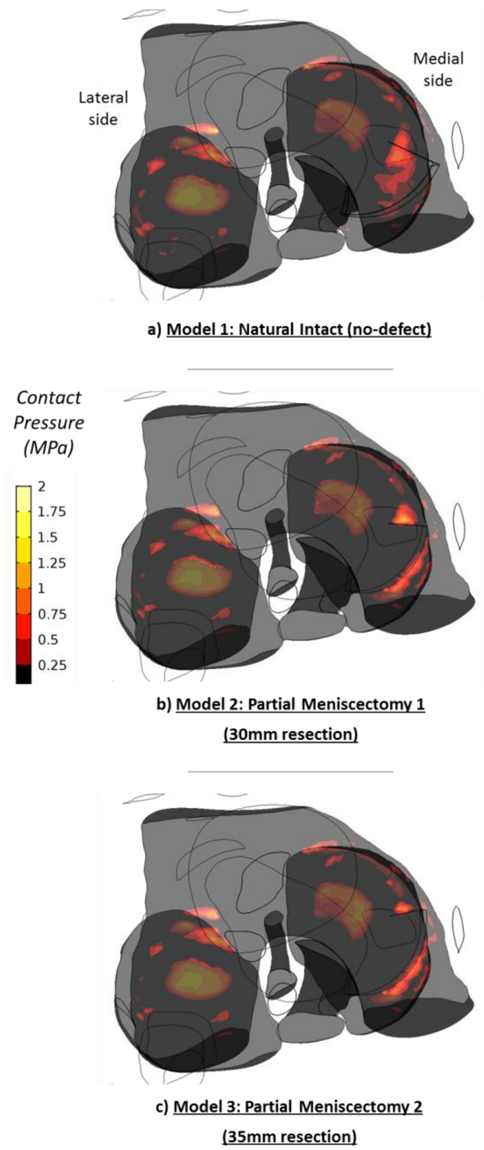

Figure 8: Contact pressure and loading patterns between the various bodies for standing load case (superior views only)

The first and third principal stresses for the menisci are presented in Figures 9 and 10, respectively. Again, as observed in Figures 7 and 8, the principal stresses in the conserving 30mm resection model are a closer match to the intact case.

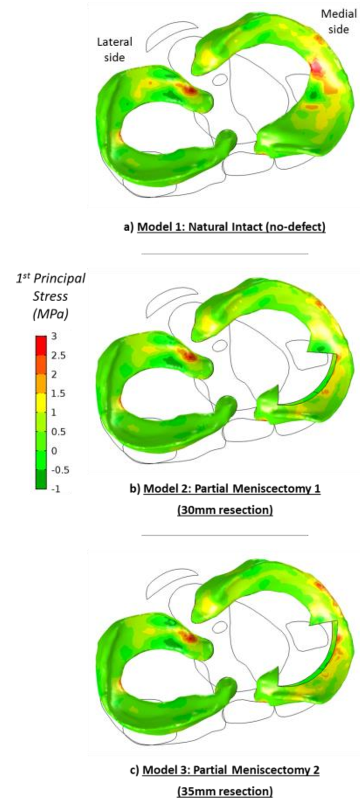

Figure 9: Menisci first principal stresses for standing load case (superior views only)

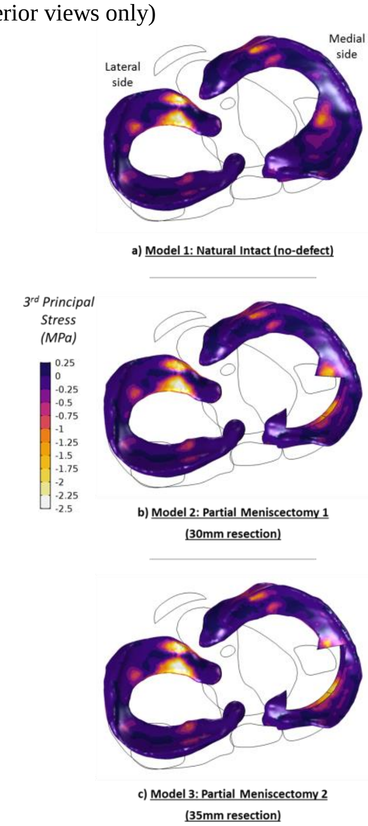

Figure 10: Menisci third principal stresses for standing load case (superior views only)

Based on the analysis plots in Figure 7 through to 10 above, the 30mm resection surgery gives a closer load response to the ideal intact case, compared to the 35mm resection surgery. This indicates that the conserving surgical optional will be better for the patient, and will help maintain a closer functional response to an intact knee. However, a quantitative assessment is required to guide surgical decisions.

Ranked Assessment

In addition to the figures presented above, the mean and maximum displacements and principal stresses, on the menisci, and contact pressures across the articulating surfaces are given in Table 2. The percentage variation of the virtual surgery model mean and maximum values relative to the intact case are also presented.

Using the maximum and average data presented in Table 2, a method of ranking the virtual surgeries was developed based on the work by Yeoman *et al.* (2009)[18]. The ranking method is used to grade the virtual surgeries and assess which is better at maintaining knee function relative to the intact case. The ranking method sums the weighted normalized parameter differences between the results from the virtual surgery models and the ideal intact reference model as follows:

$$\emptyset = \frac{\sum_i w_{\alpha_i}\left(1-\left|\frac{\alpha_i^{VS}-\alpha_i^{ND}}{\alpha_i^{ND}}\right|\right)}{\sum_i w_{\alpha_i}} \qquad (1)$$

Where, ϕ is the overall ranked value for the virtual surgery being assessed, α is the model parameter being evaluated (stress, displacement or contact pressure), superscripts VS and ND are the virtual surgery model data, and the intact (no-defect) model data, respectively. From Equation (1), it can be seen that as $\phi \rightarrow 1$, the closer the virtual surgery solution is to the intact reference model, and if $\phi = 1$, then the virtual surgery model is equal in load function to that of the intact case.

The last two rows in Table 2, present the partial ranked values for the two virtual surgery models for each parameter (α) assessed, where the partial ranked value is obtained from the part of the expression within the parentheses of Equation (1), and given by the following:

$$\emptyset_{\alpha_i} = 1 - \left|\frac{\alpha_i^{VS}-\alpha_i^{ND}}{\alpha_i^{ND}}\right| \qquad (2)$$

Again, if $\emptyset_{\alpha_i} \rightarrow 1$, the closer the virtual surgery parameter value is to the intact reference model parameter value.

Table 2: Analysis results obtained from various models

Section	Model	Contact Pressure Between Various Bodies: Medial Menisci & Tibia Cartilage Mean	Medial Menisci & Tibia Cartilage Max	Femur & Tibia Cartilage Mean	Femur & Tibia Cartilage Max	Lateral Menisci & Tibia Cartilage Mean	Lateral Menisci & Tibia Cartilage Max	Anterior-Posterior & Lateral-Medial Displacement Magnitudes: Medial Meniscus Mean	Medial Meniscus Max	Lateral Meniscus Mean	Lateral Meniscus Max	1st Principal stresses: Medial Meniscus Mean	Medial Meniscus Max	Lateral Meniscus Mean	Lateral Meniscus Max	3rd Principal stresses: Medial Meniscus Mean	Medial Meniscus Max	Lateral Meniscus Mean	Lateral Meniscus Max
Standing Load Results	Natural	0.05 MPa	0.82 MPa	0.05 MPa	1.90 MPa	0.02 MPa	1.22 MPa	0.66 mm	1.30 mm	1.05 mm	1.30 mm	0.36 MPa	8.20 MPa	0.21 MPa	5.78 MPa	-0.13 MPa	-7.35 MPa	-0.14 MPa	-10.8 MPa
	Partial Meniscectomy (30mm Resection)	0.04 MPa	1.07 MPa	0.05 MPa	1.46 MPa	0.02 MPa	1.11 MPa	0.65 mm	1.37 mm	1.11 mm	1.35 mm	0.37 MPa	9.14 MPa	0.20 MPa	6.08 MPa	-0.16 MPa	-6.35 MPa	-0.15 MPa	-10.7 MPa
	Partial Meniscectomy (35mm Resection)	0.04 MPa	1.08 MPa	0.05 MPa	1.34 MPa	0.02 MPa	1.11 MPa	0.64 mm	1.27 mm	1.04 mm	1.24 mm	0.38 MPa	10.48 MPa	0.19 MPa	6.57 MPa	-0.17 MPa	-6.25 MPa	-0.15 MPa	-10.2 MPa
Percentage variation from Natural Case	Partial Meniscectomy (30mm Resection)	-19.26 %	30.88 %	-0.63 %	-23.07 %	-9.81 %	-8.88 %	-0.41 %	5.43 %	5.44 %	3.83 %	5.16 %	11.45 %	-3.89 %	5.18 %	19.21 %	-13.66 %	5.28 %	-0.53 %
	Partial Meniscectomy (35mm Resection)	-26.04 %	32.12 %	-0.56 %	-29.37 %	-14.38 %	-9.08 %	-2.73 %	-2.26 %	-1.57 %	-4.31 %	6.26 %	27.79 %	-6.06 %	13.71 %	26.63 %	-15.01 %	8.57 %	-5.73 %
Partial Ranked Values	Partial Meniscectomy (30mm Resection)	0.81	0.69	0.99	0.77	0.90	0.91	1.00	0.95	0.95	0.96	0.95	0.89	0.96	0.95	0.81	0.86	0.95	0.99
	Partial Meniscectomy (35mm Resection)	0.74	0.68	0.99	0.71	0.86	0.91	0.97	0.98	0.98	0.96	0.94	0.72	0.94	0.86	0.73	0.85	0.91	0.94

♣ Contact pressure values are presented between their respective contact sets/pairs, and Mean contact pressure values are derived from the full surface and not just those regions in contact, thus these mean values are only useful as an indicator of overall mean contact pressures between the various models

From these partial ranked values, all but two parameters from the conserving 30mm resection model outperform the 35mm resection model. The only parameters where this is not the case, are the maximum displacement on the medical meniscus, and the mean displacement on the lateral meniscus.

Using weighting values of unity (one) for the mean parameters, and two for the maximum parameters, and substituting these, and the values in rows 1 to 3 from Table 2, into Equation (1), the overall ranked values come out as 0.90 and 0.86 for the 30mm and 35mm resection models, respectively. Thus these ranked values show that the conserving 30mm resection model is indeed better, indicating that surgical procedures should be conserving where possible, as expected.

Conclusion

A knee model has been developed to help assess the change in knee mechanics and virtual partial meniscectomy surgical options, and a quantitative virtual surgery ranking method described by Equation (1), is given.

From the results presented in Table 2, and using weightings that biased the rankings toward the maximum data parameter values, it was found that for the standing load case, the 30mm resection model presents a closer mechanical response to the ideal intact (no–defect) model. The overall ranking values obtained were 0.90 and 0.86 for the 30mm and 35mm resection models, respectively. A 3.99% increase in the ranked value (ϕ). This quantitatively shows that the conserving 30mm resection surgery is better than the 35mm resection surgery, as the closer the ranking value (ϕ) tends to unity, the closer the solution is to the ideal intact case. Thus, this virtual surgery option will better restore the function of the knee with a medial menisci defect to that of an intact knee, under the standing load conditions presented.

Although the results demonstrate that 30mm conserving resection is beneficial, only a single defect sight was assessed, where the benefits observed in conserving the menisci in this region may not necessarily be applicable at other defect sites or resections sizes. Thus, the assessment of other defect sizes and locations (e.g. medial vs. lateral and anterior vs. posterior) would be of further interest and benefit, especially if they can be correlated to clinical data.

In addition, only a small number of stress, displacement and contact pressure parameters (α) were utilized in the ranking evaluation. Future work could use additional data and parameters, such as knee joint centre of rotation, relative angular changes of the femur and tibia, and ligament stresses. These additional parameters, combined with a sensitivity analyses on the effect of the weightings could be done and correlated against clinical data and outcomes, to further develop the models and the ranking method.

This is a first effort at providing a quantitative method of comparing two surgical options, future work still needs to be done in order to validate the models and ranked method against clinical data and patient outcomes. However, the modelling technique and ranking show potential as a feasible solution for surgeons to use in a clinical setting to aid to resection options prior to surgery.

References

[1] Gray's Anatomy, The Anatomical Basis of Clinical Reference, 40th Edition (2008)

[2] Fedorov et al., 3D Slicer as an Image Computing Platform for the Quantitative Imaging Network. Magnetic Resonance Imaging. Vol. 30(9):1323-41 (2012)

[3] 3D Slicer (www.slicer.org)

[4] Tissakht and Ahmed, “Tensile Stress-Strain Characteristics of the Human Meniscal Material,” Journal of Biomechanics, Vol. 28 (4):411-422 (1995).

[5] Yong Bae et al., “Biomechanical analysis of the effects of medial meniscectomy on degenerative osteoarthritis”, Medical & Biological Engineering & Computing, Vol. 50 (1):53–60 (2012)

[6] F. Reisse, Effect of Malalignement of Knee Joint Contact Mechanics, PhD Thesis, Anglia Ruskin University (2014)

[7] Mootanah et al., Development and validation of a computational model of the knee joint for the evaluation of surgical treatments for osteoarthritis, Computer Methods in Biomechanics and Biomedical Engineering, Vol. 17: 1502–1517(2014)

[8] Mononen et al., Effects of Radial Tears and Partial Meniscectomy of Lateral Meniscus on the Knee Joint Mechanics during the Stance Phase of the Gait Cycle—A 3D Finite Element Study, Journal of Orthopaedic Research, Vol. 31(8):1208–1217(2013)

[9] Westermann et al., Effect of ACL Reconstruction Graft Size on Simulated Lachman Testing: A Finite Element Analysis, The Iowa Orthopaedic Journal Vol. 33:70–77 (2013)

[10] Kiapour et al., Finite Element Model of the Knee for Investigation of Injury Mechanisms: Development and Validation, Journal of Biomechanical Engineering, Vol. 136 (2014)

[11] Pena et al., A Three-Dimensional Finite Element Analysis of the Combined Behavior of Ligaments and Menisci in the Healthy Human Knee Joint. Journal of Biomechanics, Vol. 39(9), pp 1686–1701 (2006)

[12] Carey et al., Subject-Specific Finite Element Modeling of the Tibiofemoral Joint Based on CT, Magnetic Resonance Imaging and Dynamic Stereo-Radiography Data in Vivo, Journal of Biomechanical Engineering, Vol. 136 (2014)

[13] Galbusera et al., “Material Models and Properties in the Finite Element Analysis of Knee Ligaments: A Literature Review.” Frontiers in Bioengineering and Biotechnology Vol. 2 (2014).

[14] Sanford et al., Hip, Knee and Ankle Joint Forces in Healthy Weight, Overweight and Obese Individuals During Walking-Computational Biomechanics for Medicine. Springer, New York, NY (2014)

[15] Della Croce et al., Human movement analysis using stereo photogrammetry Part 4: assessment of anatomical landmark misplacement and its effects on joint kinematics, Gait and Posture, Vol. 21:226–237 (2005)

[16] Kadaba et al., Measurement of Lower Extremity Kinematics During Level Walking, Journal of Orthopaedic Research Vol. 8(3):383-92 (1990)

[17] Basic Biomechanics of the Musculoskeletal System, Edited by Margareta Nordin DirSci & Victor H. Frankel MD PhD (4th Edition), Lippincott Williams & Wilkins (2012)

[18] Yeoman *et al.*, The Use of Finite Element Methods and Genetic Algorithms in Search of an Optimal Fabric Reinforced Porous Graft System, Annals of Biomedical Engineering, Vol. 37(11): 2266—2287(2009)